Single-pass Process of Square Butt Joints without Edge Preparation using Hot-wire Gas Metal Arc Welding

Nattasak Suwannatee and Motomichi Yamamoto *

Posted Date: 9 May 2023

doi: 10.20944/preprints202305.0633.v1

Keywords: hot-wire; gas metal arc welding; single-pass welding; lower energy consumption welding

Article

Single-Pass Process of Square Butt Joints without Edge Preparation Using Hot-Wire Gas Metal Arc Welding

Nattasak Suwannatee and Motomichi Yamamoto *

Graduate School of Advanced Science and Engineering, Hiroshima University, Higashi-Hiroshima 730-0046, Japan; d205056@hiroshima-u.ac.jp

* Correspondence: motoyama@hiroshima-u.ac.jp; Tel.: +81-82-424-7815

Abstract: This paper presents a novel approach of welding thick steel plates that offers time and energy savings compared with conventional techniques. The combination of gas metal arc welding (GMAW) and hot-wire technology simplifies the joint configuration and enhances the process tolerance. In this study, a square butt joint was prepared with as-cut edges and a thickness of 15 mm. The relationship between the welding current and the deposition rate of solo GMAW showed limitations and low process tolerance. Increasing the welding current led to a larger deposited volume with unnecessary weld penetration. An independent deposition volume due to hot-wire insertion was used to improve process tolerance. This approach provided an additional volume without increasing the welding current and reduced unnecessary penetration. With optimized parameters, full-penetration single-pass welding was achieved. Compared with the formation of a typical single-v butt joint at a similar welding speed of 30 cm/min, the proposed process reduced the minimum arc time and power consumption by approximately 83% and 62%, respectively. Moreover, a single pass at a travel speed of 60 cm/min was achieved with approximately 91% and 81% less arc time and power consumption, respectively. In summary, the combined process simplifies the joint configuration, enables full-penetration single-pass welding, and reduces time and energy requirements.

Keywords: hot-wire; gas metal arc welding; single-pass welding; lower energy consumption welding

1. Introduction

Traditional welding processes, including gas metal arc welding (GMAW), necessitate the preparation of grooves (edges) to ensure the accessibility of a welding torch and produce high-quality welds without defects. However, the joint preparation process is not only time consuming but also expensive [1,2]. Moreover, a large groove area requires many welding passes and/or high welding current in GMAW to achieve the desired deposition volume [3–5]. Although there are highly efficient welding processes with larger deposition volumes, such as submerged arc welding [6,7] and tandem arc welding [8,9], they often require high welding currents to achieve high deposition rates, which may deteriorate joint properties through grain coarsening adjacent to the fusion boundary in the heat-affected zone [10,11].

Several researchers have proposed combining hot-wire insertion with several main heat sources, such as in hot wire with laser welding [12–15] and hot wire with ultra-high-speed gas tungsten arc welding [16], which obviously have the benefits of hot-wire insertion. Although the deposition volume can be increased, the groove (edge) preparation and a more precious joint configuration are required. The combination of GMAW and hot-wire feeding has since been proposed and used to increase productivity and process tolerances [17,18]. In a recent study, the full penetration of a butt-joint single-V groove in a 36-mm-thick steel plate was achieved with only four weld passes [19].

Preprints (www.preprints.org) | NOT PEER-REVIEWED | Posted: 9 May 2023 doi:10.20944/preprints202305.0633.v1

Moreover, the study revealed the precedence of molten metal under the limitation of the total deposition volume, which depended on the bead width (gap size) of the butt-joint single-V groove weld. Another study suggested that increasing the welding speed not only reduced heat input but also increased the controllability of the arc at high current and affected the weld bead shape [20]. Notably, hot-wire GMAW has promising controllability of the molten pool formation with less required heat input. The authors thus propose an optimized hot-wire GMAW for creating a single-pass weld on thick steel plates without edge preparation.

The present study investigates the limitations of conventional GMAW and optimizes the welding conditions of hot-wire GMAW to achieve single-pass welding on a square butt joint of 15-mm-thick steel plates. To achieve this goal, the effect of the hot-wire fraction on the quality of the welded joint is investigated. The welding quality is monitored using a high-speed camera, and the weld bead geometry on an etched cross-section is measured in detail. Furthermore, the power consumption and arc time are calculated and compared with those of conventional GMAW to demonstrate the energy savings and increased productivity associated with hot-wire GMAW.

2. Materials and Methods

2.1. Materials

A square butt joint of JIS-G3101-SS400 with as-cut surfaces having a length of 350 mm, width of 80 mm, and thickness of 15 mm was assembled with a 9-mm-thick backing plate for the experiment as shown in Figure 1. Two root gaps, 5 and 10 mm in width, were used. The filler metal used for GMAW was a JIS-Z3312-YGW11 (G49A0UC11) solid wire with a diameter of 1.4 mm, whereas the same filler wire but with a different diameter of 1.2 mm was used for the hot wire. Chemical compositions of the materials used in the experiment are given in Table 1.

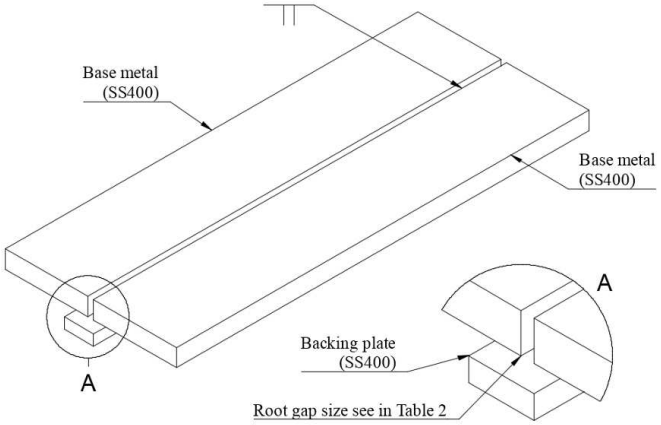

Figure 1. Joint configurations.

Table 1. Chemical compositions of G3101-SS400 and Z3312-YGW11 (wt%).

Element	C	Si	Mn	P	S	Ti+Zr	Fe
Base metal	0.26	0.40	-	0.04	0.05	-	Bal.
Filler metal	0.08	0.51	1.10	0.01	0.01	0.05	Bal.

2.2. Experimental Setup

Figure 2a is a schematic of the experimental setup of the solo GMAW process. One-hundred-percent CO_2 was used as the shielding gas. The GMAW torch was placed perpendicular to the welding direction and backing plate. Figure 2b shows the combination of the GMAW and hot wire with a 10-mm delay of the hot-wire feeding position in the welding direction. The distance from the contact tip to workpiece and the distance of the power supply were maintained at 30 and 100 mm, respectively. The hot-wire feeding angle was fixed at 70 degrees relative to the backing plate.

Preprints (www.preprints.org) | NOT PEER-REVIEWED | Posted: 9 May 2023 doi:10.20944/preprints202305.0633.v1

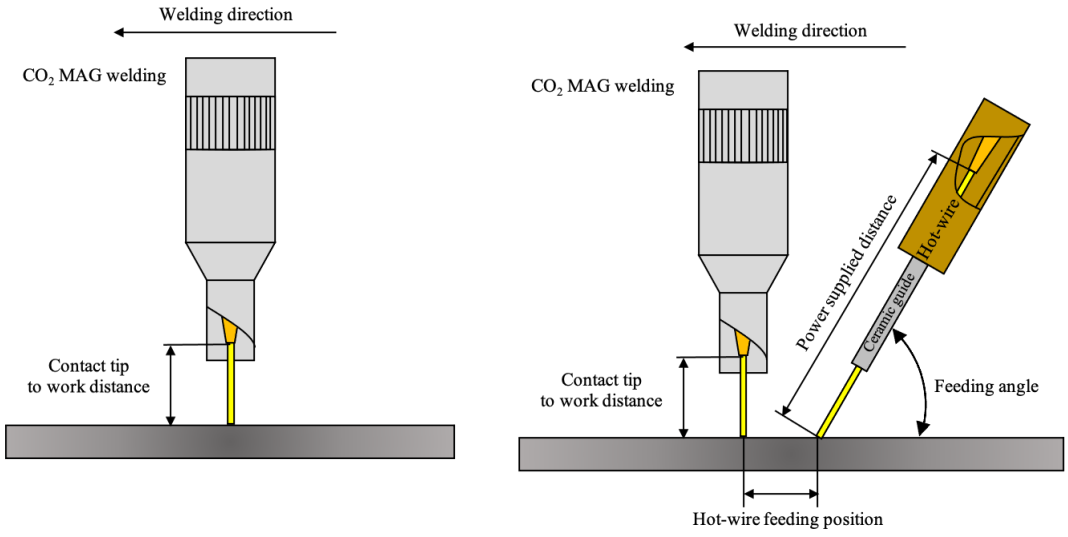

(**a**) (**b**)

Figure 2. Welding experimental setups: (**a**) schematic of solo GMAW and (**b**) schematic of hot-wire GMAW.

Initially, GMAW was performed without hot-wire insertion to determine process capabilities and limitations. Table 2 gives the welding conditions for the solo GMAW experiment. To investigate the effect of the welding current on the weld bead profile and arc position on the square butt joint, the welding current was increased from 300 to 500 A in intervals of 50 A while other parameters, such as an arc voltage of 38 V and travel speed of 30 cm/min, were held constant under the initial condition with the 5-mm gap. The wire feeding speed (WFS) was measured and the deposition rate of the GMAW was calculated at the different applied welding currents. Subsequently, additional experiments for a larger gap of 10 mm and a constant travel speed of 30 cm/min (larger gap condition) and a faster welding speed of 60 cm/min and constant gap size of 5 mm (faster speed condition) were conducted to determine the limitations of the GMAW process.

Table 2. Conditions of solo GMAW.

Parameters	Initial condition	Larger gap condition	Faster speed condition
Gap size, mm	5	10	5
Travel speed, cm/min	30		60
Welding current, A	300-500		
Arc voltage, V	38		
Gas flow rate, L/min	25		
Contact tip to work distance, mm	30		

The arc phenomenon and molten pool formation were observed using a high-speed camera. A band pass filter with a transmission wavelength of 810 ± 10 nm was attached to an optical lens. A shutter speed of 1/1000 s and a frame rate of 500 fps were adopted. The resulting welds were cross-sectionally cut, polished, and etched with 3% nitric acid. Subsequently, the weld geometry was observed. Figure 3 shows measured parameters of the weld geometry, such as the fusion area (A_f), depth of penetration (D_p), maximum width (W_{max}), and height (H_{wmax}), on the obtained welded cross-section.

Preprints (www.preprints.org) | NOT PEER-REVIEWED | Posted: 9 May 2023 doi:10.20944/preprints202305.0633.v1

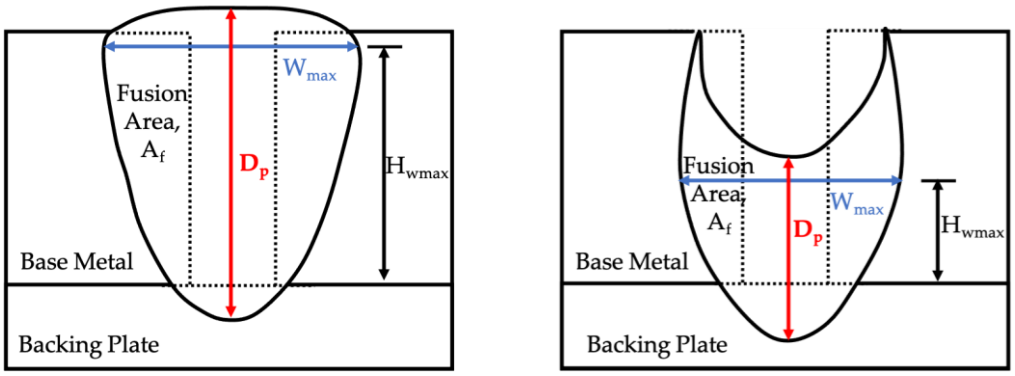

Figure 3. Measured parameters on the obtained welded cross-section: (**a**) weld geometry parameters for the underfill condition and (**b**) weld geometry parameters for the full-penetration condition.

2.3. Calculation of the Optimal Hot-wire Current

The hot-wire must be smoothly and continuously fed into the molten pool to obtain an exact deposition volume. Several studies have provided simple calculations with which to derive an optimal hot-wire current that relates to the hot-wire feeding speed [15–17]. The power supply distance of 100 mm was divided into segments of 0.1 mm. The temperature increment on a segment (ΔT) in degrees Celsius is given by

$$\Delta T = \frac{Q}{\pi \times \left(\frac{d}{2}\right)^2 \times L \times C(T) \times m(T)}, \quad (1)$$

where d is the diameter of the hot wire in mm, C(T) is the temperature-dependent specific heat in J/kg·ºC, and m(T) is the temperature-dependent density in kg/m^3. Q is the net heat increase calculated as

$$Q = R(T) \times I^2 \times D \times 60 \times \frac{L}{V_{fh}} - h \times A \times (T_w - T_a), \quad (2)$$

where I is the hot-wire current in A, D is the duty cycle of the wire heating (normally set at 50%), V_{fh} is the hot wire feeding speed in m/min, h is the comprehensive heat loss coefficient in W/m^{2}K, T_w is the temperature of the filler wire in °C, and T_a is the air temperature in °C. R(T) is the temperature-dependent resistance of the filler material in Ω given as

$$R(T) = \frac{(R_C + \rho(T) \times L)}{\pi \times r^2}, \quad (3)$$

where R_c is the contact resistant in Ω and ρ(T) is the temperature-dependent specific electrical resistivity in Ω·m

Substituting equations (2) and (3) into equation (1), a simple equation is derived to calculate the temperature increment on the hot-wire segment:

$$\Delta T = \frac{I^2}{V_f} \times \frac{60 \times L \times D \times (R_c + \rho(T))}{\pi^2 \times \left(\frac{d}{2}\right)^2 \times C(T) \times m(T)} - \frac{h \times (T_w - T_a)}{C(T) \times m(T) \times L}. \quad (4)$$

Equation (4) is used to obtain the optimal hot-wire current when the wire temperature at the tip equals the melting temperature.

2.4. Definition of the hot-wire fraction

The hot-wire insertion volume is used as an independent deposition metric and increased to increase the total deposition volume. The hot-wire fraction representing this effect is expressed as

Preprints (www.preprints.org) | NOT PEER-REVIEWED | Posted: 9 May 2023 doi:10.20944/preprints202305.0633.v1

$$\%HW = \frac{WFS_{HW}}{(WFS_{HW} + WFS_{GMAW})} \times 100, \quad (5)$$

where %HW is the hot-wire fraction in percent, WFS_{HW} is the hot-wire feeding speed in cm/min, and WFS_{HW} is the wire feeding speed of GMAW in cm/min.

2.5. Calculation of the Power Consumption

A data acquisition system operating at 5000 Hz was used to record the welding current in A, arc voltage in V, hot-wire current in A, and hot-wire voltage in V. The total power consumption is

$$P_{total} = \frac{(P_{GMAW} + P_{HW})}{\text{travel speed}}, \quad (6)$$

where

$$P_{GMAW} = \frac{(I_{GMAW1} \times V_{GMAW1}) + (I_{GMAW2} \times V_{GMAW2}) + \ldots + (I_{GMAWn} \times V_{GMAWn})}{n}, \quad (7)$$

$$P_{HW} = \frac{\left(\sqrt{I_{HW1}^2} \times \sqrt{V_{HW1}^2}\right) + \left(\sqrt{I_{HW2}^2} \times \sqrt{V_{HW2}^2}\right) + \ldots + \left(\sqrt{I_{HWn}^2} \times \sqrt{V_{HWn}^2}\right)}{n}. \quad (8)$$

Here, P is the power used in GMAW and hot wiring (kW), I is the welding current (A), V is the arc voltage (volt), and n is the number of samples.

3. Capability of GMAW

3.1. Relationship between the Welding Current and WFS

Figure 4 presents the relationship between the welding current and measured WFS in solo GMAW. It is seen that despite fluctuations in the welding current, the constant-voltage GMAW welding power source maintains a nearly constant arc length, resulting in a proportional relationship between the welding current and WFS [21]. This result reveals the necessity of increasing the welding current to obtain a larger deposition volume, leading to more heat input to the joint and ultimately grain coarsening adjacent to the fusion line and worse joint properties. This highlights the limitation of conventional GMAW in achieving desired deposit volumes and emphasizes the importance of independent supplemental deposition techniques that do not rely on the welding current.

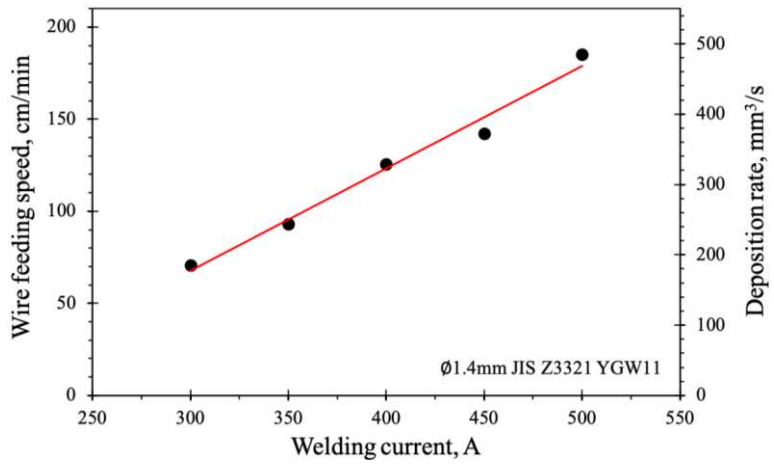

Figure 4. Relationship between the welding current, wire feeding speed, and deposition rate.

3.2. Arc Phenomenon, Bead Appearance, and Weld Geometry

The study examined the effect of varying the welding current from 300 to 500 A under three different sets of conditions, as previously given in Table 2. Figure 5a presents the captured high-speed

Preprints (www.preprints.org) | NOT PEER-REVIEWED | Posted: 9 May 2023 doi:10.20944/preprints202305.0633.v1

images, weld bead appearances, and cross-sections when conventional GMAW was applied to the 5-mm gap of the square butt joint with a welding speed of 30 cm/min (i.e., the initial set of conditions). The captured high-speed images show different arc positions relating to the height of the molten pool. As the welding current was increased, the arc moved upward in the depth direction, resulting in a shorter stick-out distance of the filler metal. A sound weld bead shape could not be achieved under the initial conditions. A welding current lower than 400 A resulted in an insufficient depth of penetration with incomplete fusion; i.e., underfilling of the weld bead with a cone-shaped fusion area. However, increasing the welding current helped to overcome the incomplete fusion, changing the shape of the fusion area from a cone to a rectangle.

Figure 5b illustrates that increasing the welding current not only provided a larger deposition volume but also affected the weld bead geometry. Increasing the welding current resulted in a narrower maximum weld width (W_{max}) and larger depth of penetration (D_P). The height of the maximum weld width position (H_{wmax}) represents the arc position in this experiment, and Figure 5(b) shows that the arc was positioned deeper in the thickness direction as the welding current increased. The depth-to-width (D/W) ratio has been used to explain the change in the shape of a weld profile and its sensitivity to hot cracking [22]. A welding current between 400 to 500 A provided similar fusion area sizes (A_f) but with a large difference in the D/W ratio. In general, a high D/W ratio in solo GMAW led to solidification cracking and a non-smooth bead appearance as shown in Figure 5(a).

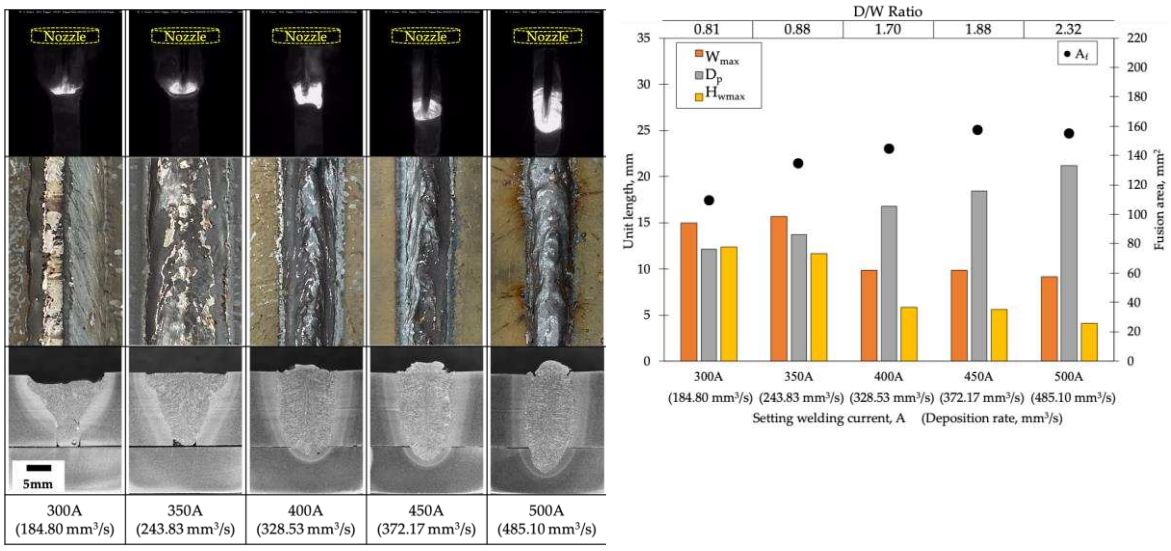

(**a**) (**b**)

Figure 5. Effect of the welding current in solo GMAW for a 5-mm gap and a welding speed of 30 cm/min: (**a**) arc behavior, weld bead appearance, and cross-sectional analysis and (**b**) weld profile measurement.

In the following welding experiments, similar deposition rates were achieved for the same welding speed of 0.3 m/min, but with the root gap increasing from 5 to 10 mm. Figure 6a presents the images captured during welding, the appearances of weld beads, and the cross-sections obtained for comparable deposition rates. The larger root gap allowed the generation of a bigger molten pool at the root, even when applying the lowest welding current (300 A) in this experiment. Despite only increasing the gap, a deposition volume sufficient for single-pass welding could not be achieved, although the precedence of molten metal was suppressed. Figure 6b shows that H_{wmax} decreased as the welding current increased, and the arc was positioned deeply in the thickness direction, leading to a high D/W ratio. However, the yellow bar indicates only a positive value, which means that the arc was in the region of the backing plate. When the welding current exceeded 450 A, the obtained D_P exceeded the thickness of the base metal. These results suggest that if the arc can be shifted to the upper side of the joint, unnecessary penetration can be reduced, and a single-pass welded joint can be obtained.

Preprints (www.preprints.org) | NOT PEER-REVIEWED | Posted: 9 May 2023 doi:10.20944/preprints202305.0633.v1

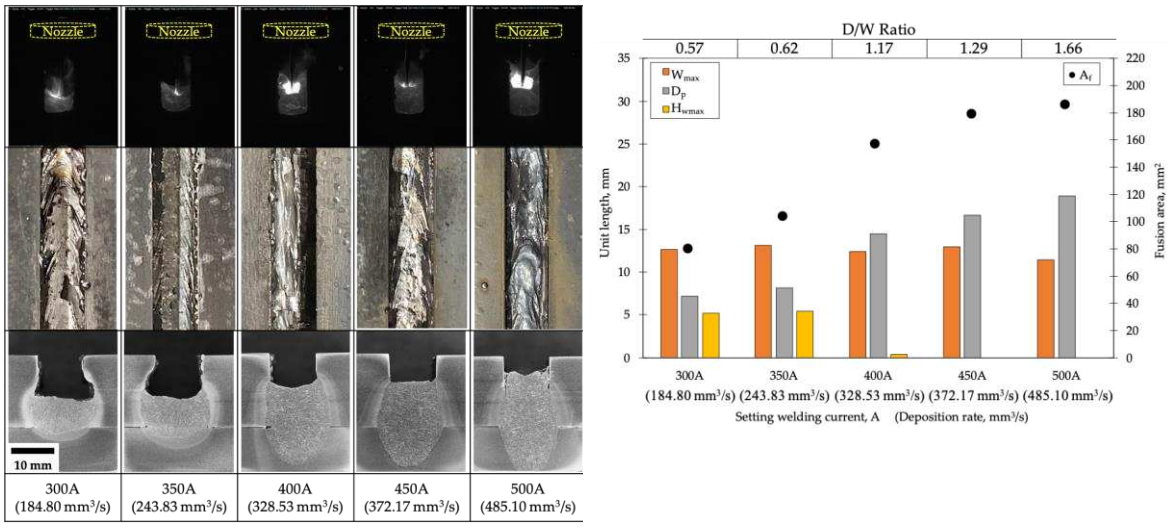

(**a**) (**b**)

Figure 6. Effects of the welding current for a 10-mm gap and a travel speed of 30-cm/min: (**a**) arc behavior, weld bead appearance, and cross-sectional analysis and (**b**) weld profile measurement.

Another experiment was conducted where a similar deposition rate was used for the 5-mm root gap but the welding speed was increased from 30 to 60 cm/min. Figure 7a presents the captured images, weld bead appearances, and macro-etched cross-sections. When using a welding current of 300 A, the molten pool was generated at the upper side of the gap, leading to incomplete fusion on the bottom side. Thus, the D/W ratio and D_p could not be determined under the conditions. The welding speed is the most dominant factor of heat input [10,21]. The halving of the heat input due to the doubling of the welding speed resulted in a smaller molten pool as seen in the captured images. In this experiment, all welding currents provided an underfill weld bead (insufficient deposition volume) and poor weld geometry (high D/W ratio), which resulted in solidification cracking at the center of the weld metal perpendicular to the direction of solidification. Figure 7b shows a similar trend for H_{wmax}, which decreased with increasing welding current compared with both prior experiments. A similar behavior was observed for W_{max}, which decreased with increasing welding current.

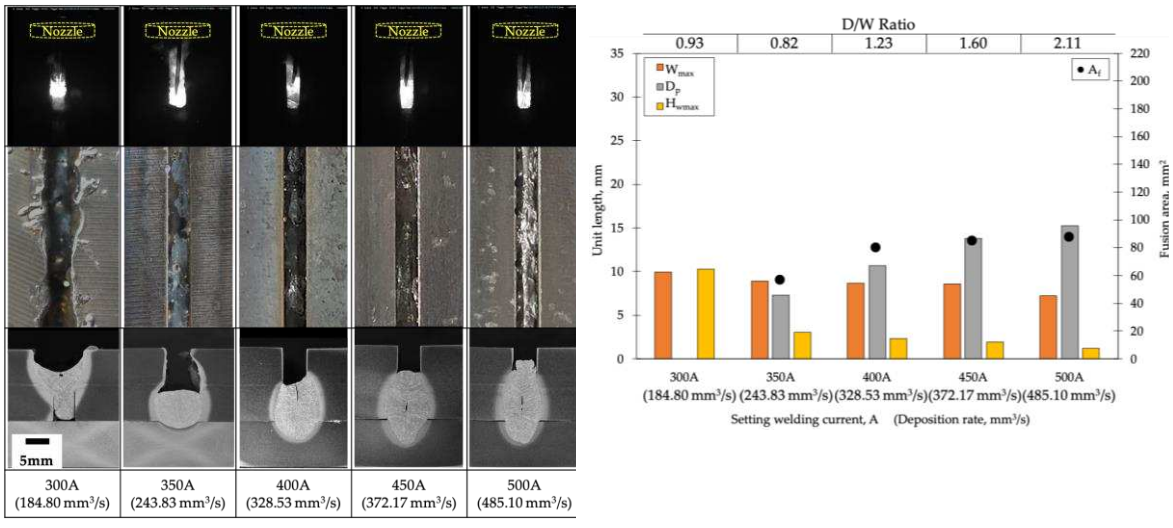

(**a**) (**b**)

Figure 7. Effects of the welding current for a 5-mm gap and a travel speed of 60-cm/min: (**a**) arc behavior, weld bead appearance, and cross-sectional analysis and (**b**) weld profile measurement.

In summary, the three experiments revealed the limitation of conventional GMAW, namely that the deposition rate is restricted by the welding current. This series of experiments showed that single-

Preprints (www.preprints.org) | NOT PEER-REVIEWED | Posted: 9 May 2023 doi:10.20944/preprints202305.0633.v1

pass welding on a square butt joint of 15-mm-thick steel plates could not be achieved through solo conventional GMAW. To overcome this drawback, an independent additional volume from hot wire was used in further investigation.

4. Capability of the Hot-wire GMAW Process

4.1. Relationship between the Hot-wire Current and Hot-wire Feeding Speed

To ensure continuous hot-wire feeding, the appropriate hot-wire current was determined according to the wire feeding speed. Figure 8 depicts the behaviors observed for a 1.2-mm-diameter hot wire fed at 10 m/min. The measured optimal hot-wire current indicated by red circles provided an appropriate feed. An insufficient hot-wire current, as indicated by the red cross, can result in the formation of unmelted filler metal in a molten pool, which can push the molten metal forward. Meanwhile, an excessive hot-wire current, as shown by the red square, can lead to the interruption and meltdown of wire feeding and thus negatively affect the deposition rate and weld quality. The correlation between the optimal hot-wire current and hot-wire feeding speed was established and used in the subsequent experiment. This correlation is essential for achieving a stable wire feed and maintaining the desired weld quality in single-pass welding.

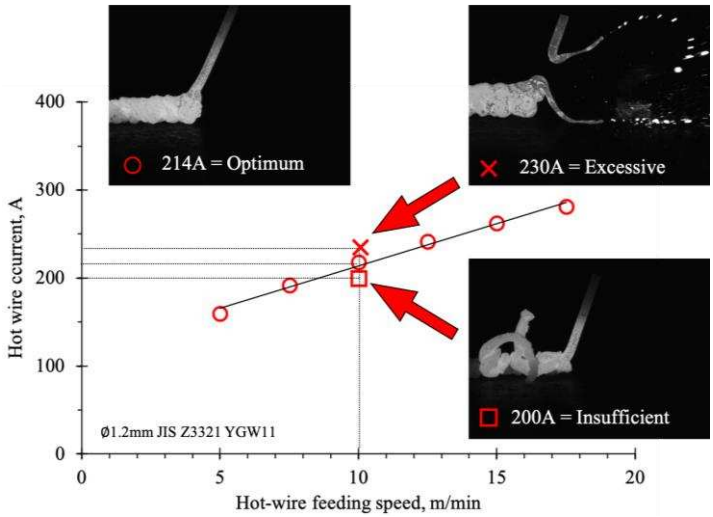

Figure 8. Correlation between the optimal hot-wire current and hot-wire feeding speed.

4.2. Effect of the Hot-wire Fraction on Weld Formation and Obtained Weld Geometry

Hot-wire insertion can be controlled independently from the welding current as an independent fraction volume, greatly affecting the total deposition volume. The hot-wire fraction was increased to achieve sufficient deposition rates for the larger gap and faster welding speed conditions. For conventional GMAW in the prior session, a welding current of 500 A resulted in an excessive deposition volume and an overly strong and unstable arc, whereas a welding current below 400 A did not provide a sufficient deposition volume even with hot-wire insertion. Therefore, a constant welding current of 450 A was chosen to optimize the single-pass welding conditions. The hot-wire fraction was varied to analyze the weld pool formation and the obtained weld geometry. Increasing the fraction in the total deposition volume enabled single-pass welding under the specified conditions.

Figure 9a shows the images captured during welding and cross-sections for a 10-mm gap and a welding speed of 30 cm/min. The increase in the hot-wire fraction lifted upward the central position of the weld bead toward the plate surface, resulting in the generation of the molten pool on the upper side of the groove. Although the total deposition volume increased with the hot-wire fraction, the arc force was sufficient to maintain the molten pool shape and penetration in the bottom region. Figure 9b presents parameters of the measured geometry of the weld bead. W_{max} and D_p remained

Preprints (www.preprints.org) | NOT PEER-REVIEWED | Posted: 9 May 2023 doi:10.20944/preprints202305.0633.v1

approximately constant whereas H_{wmax}, representing the arc position, increased with the deposition rate. The D/W ratios emphasized the similarity of the weld geometry. The hot-wire fraction can thus be used to adjust the position of the weld bead and reduce unnecessary penetration. Sound joint conditions were achieved at a hot-wire fraction of 43.18%.

A similar experiment was conducted for a 5-mm gap and a travel speed of 60 cm/min. Figure 10a shows that the position of the arc changed as the hot-wire fraction increased. For a constant GMAW fraction, the arc shifted toward the top surface with an increase in the hot-wire fraction up to 43.18%. This is strong evidence that the hot-wire fraction can be used to control the arc position and enlarge the process tolerance. Thus, single-pass welding of a 15-mm square butt joint could be achieved even at a travel speed of 60 cm/min. Figure 10b illustrates a trend in the weld geometry similar to that in the prior experiment, with an obvious increase in H_{wmax} with the deposition rate. Notably, solidification cracking that first occurred when conventional GMAW was applied shifted position as the hot-wire fraction increased. In addition, the crack disappeared at a hot-wire fraction of 43.18%, and the conditions provided a sound joint without defects.

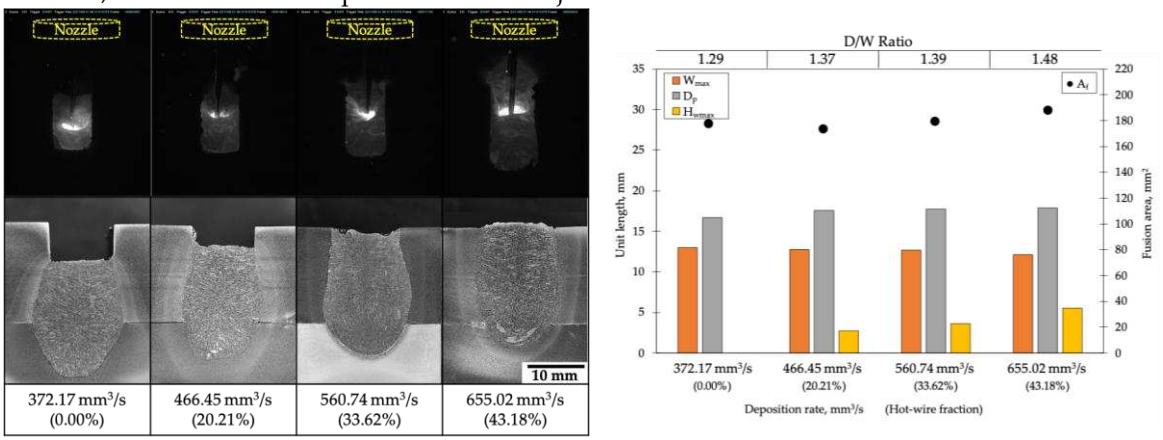

(**a**) (**b**)

Figure 9. Effects of the hot-wire fraction for a 10-mm gap and travel speed of 30 cm/min: (**a**) arc behavior and cross-sectional analysis and (**b**) weld profile measurements.

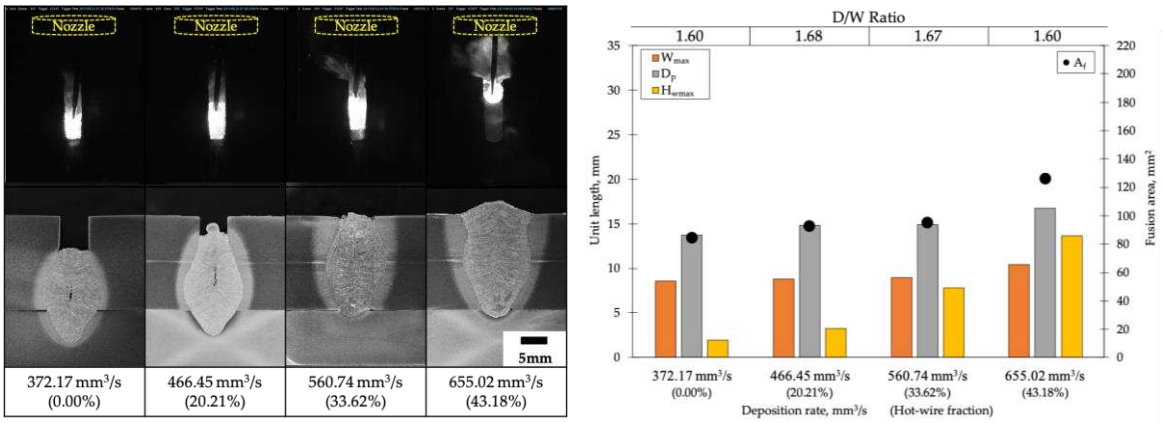

(**a**) (**b**)

Figure 10. Effects of the hot-wire fraction for a 5-mm gap and travel speed of 60 cm/min: (**a**) arc behavior and cross-sectional analysis and (**b**) weld profile measurements.

5. Power Consumption and Productivity

Figure 11 presents a reduction in the arc time when using hot-wire insertion compared with using conventional GMAW. The adoption of the proposed process resulted in an 83.3% reduction in the arc time at the same travel speed. At a travel speed of 60 cm/min, single pass welding had a remarkable 91.7% reduction in arc time. These reductions in arc time, represented by gray bars in the

Preprints (www.preprints.org) | NOT PEER-REVIEWED | Posted: 9 May 2023 doi:10.20944/preprints202305.0633.v1

figure, can be considered a measure of production efficiency. The use of hot-wire insertion led to a notable increase in production efficiency. By reducing the required number of weld passes from six to one, production efficiency increased by a factor of approximately 5 at the same travel speed of 30 cm/min. Under optimized conditions of a 5-mm gap and a travel speed of 60 cm/min, the production efficiency of the proposed method was approximately 11 times that of the conventional GMAW. In addition, the proposed welding process is suitable for a square groove without any preparation and with a large gap variation.

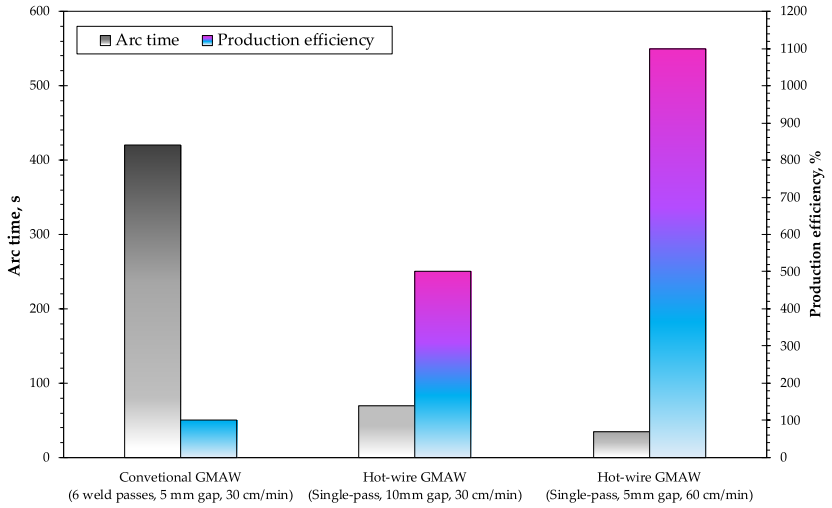

Figure 11. Comparison of the arc time and power consumption between conventional GMAW and the proposed hot-wire GMAW.

Figure 12 presents the relationship between the deposition rate and power consumption for various welding processes. Conventional GMAW has limited process tolerance, with the deposition volume depending on the applied welding current and filler metal diameter [16,20]. Proposed high-current CO_2 arc welding has a high deposition rate but requires power consumption similar to that required by submerged arc welding (SAW) [3]. Increasing the diameter of the filler metal improves the deposition rate of SAW [8] but inevitably results in high power consumption. However, the adoption of hot-wire insertion led to a reduction in power consumption of 52% compared with SAW for a similar deposition volume. The proposed method is thus a sustainable-development way of achieving high deposition volume while minimizing power consumption. The optimized hot-wire current and fraction enable stable hot-wire feeding for the arc and maximize the deposition rate, making the proposed method promising for welding applications that require high productivity and energy efficiency.

Preprints (www.preprints.org) | NOT PEER-REVIEWED | Posted: 9 May 2023 doi:10.20944/preprints202305.0633.v1

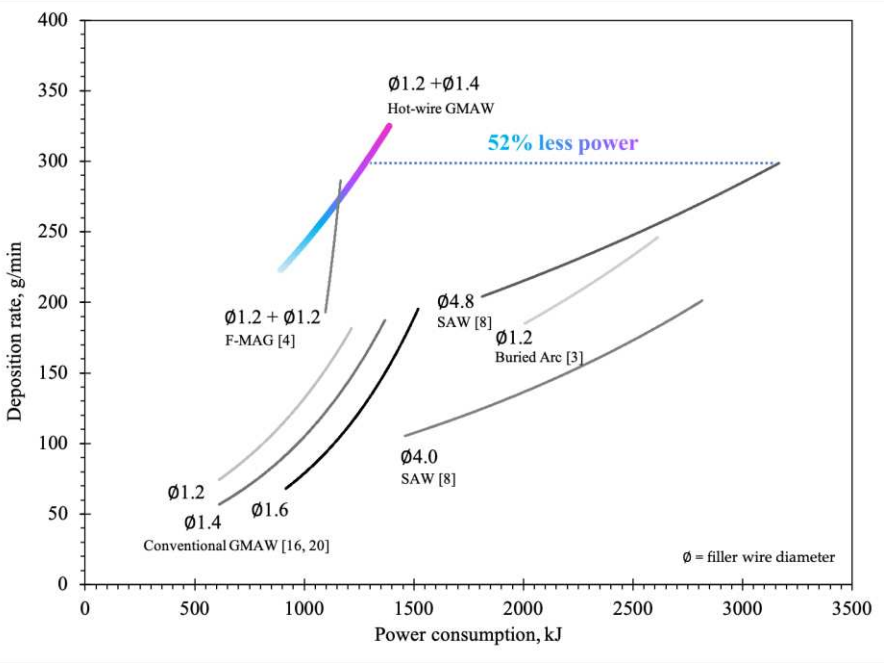

Figure 12. Relationship between the deposition rate and power consumption in various welding processes.

This study investigated the limitation of conventional GMAW and the use of the hot-wire fraction as a parameter for controlling the desired position of the weld metal. The results of the study show that the new approach forms a promising sound joint when optimized conditions are applied. The main results and conclusions of the study are as follows.

1. The limited process tolerance of GMAW in achieving single pass welding was shown. Obtaining a greater deposition volume inevitably requires high heat input to the joint.
2. As the hot-wire fraction increases, the molten pool tends to form on the upper side of the joint. Unnecessary penetration is reduced, and a desired arc position is obtained, particularly for large gaps and high travel speeds.
3. The simple joint configuration can be used to achieve single pass welding using the proposed process.
4. The independent deposition volume due to hot-wire insertion increases the total deposition volume without requiring more welding current. Single-pass welding at a welding speed of 60 cm/min resulted in an 81.25% decrease in power consumption.
5. The productivity increases with decreasing arc time. The proposed approach requires 91.67% less arc time compared with conventional GMAW.
6. The use of the hot wire reduces the occurrence of solidification cracks in the welded joint.

However, further research is needed to optimize the hot-wire fraction and other process parameters and thus achieve the best possible welding results for specific applications.

Author Contributions: Conceptualization, N.S. and M.Y.; methodology, N.S.; software, N.S.; validation, N.S. and M.Y.; investigation, N.S.; resources, M.Y.; data curation, N.S.; writing—original draft preparation, N.S.; writing—review and editing, N.S. and Y.M.; visualization, N.S.; supervision, M.Y.; project administration, M.Y.; funding acquisition, M.Y. All authors have read and agreed to the published version of the manuscript.

Funding: This work was supported by JSPS KAKENHI Grant Number 21H01548.

Data Availability Statement: Not applicable.

Acknowledgments: We express our sincere gratitude to Kanon Nakamura for their invaluable contributions and support throughout this project.

Conflicts of Interest: The authors declare no conflict of interest.

References

1. Masmoudi, F., Bouaziz, Z. Hachicha, W. Computer-aided cost estimation of weld operations. *Int. J. Adv. Manuf. Technol*. **2007** 33, 298–307. https://doi.org/10.1007/s00170-006-0463-0
2. Chayoukhi, S., Bouaziz, Z., Zghal, A. Cost estimation of joints preparation for GMAW welding process using feature model, *J. Mater. Process. Technol*. **2008**, 199.1-3, 402-411. https://doi.org/10.1016/j.jmatprotec.2007.08.024
3. Baba, H., Era, T., Ueyama, T., Tanaka, M. Single pass full penetration joining for heavy plate steel using high current GMA process. *Weld World* **2017**, 61, 963–969. https://doi.org/10.1007/s40194-017-0464-7
4. Tsuyama, T., Yuda, M., Nakai, K.: Effects of hot wire on mechanical properties of weld metal using gas-shield arc welding with CO2 gas, *Weld World* **2014**, 58, 77-83. https://doi.org/10.1007/s40194-013-0094-7
5. Wu, C.S., Hu, Z.H. & Zhong, L.M. Prevention of humping bead associated with high welding speed by double-electrode gas metal arc welding. *Int J Adv Manuf Technol*. **2012**, 63, 573–581. https://doi.org/10.1007/s00170-012-3944-3
6. Gunaraj, V., Murugan, N. Application of response surface methodology for predicting weld bead quality in submerged arc welding of pipes. *J. Mater. Process. Technol*. **1991**, 88.1-3, 266-275. https://doi.org/10.1016/S0924-0136(98)00405-1
7. Murugan, N., Gunraj, V. Prediction and control of weld bead geometry and shape relationships in submerged arc welding of pipes, *J. Mater. Process. Technol*. **2005**, 168-3, 478-487. https://doi.org/10.1016/j.jmatprotec.2005.03.001
8. Tsuyama, T., Nakai, K. Tsuji, T. Development of submerged arc welding method using hot wire. *Weld World*. **2014**, 58, 713–718. https://doi.org/10.1007/s40194-014-0153-8
9. Ueyama, T., Ohnawa, T., Tanaka, M., & Nakata, K.: Effects of torch configuration and welding current on weld bead formation in high speed tandem pulsed gas metal arc welding of steel sheets, *Sci. Technol. Weld. Join*. **2005**, 10-6, 750-759. https://doi.org/10.1179/174329305X68750
10. Ueyama, T., Ohnawa, T., Tanaka, M., & Nakata, K.: Occurrence of arc interaction in tandem pulsed gas metal arc welding, *Sci. Technol. Weld. Join*. **2007**, 12-6, 523-529. https://doi.org/10.1179/174329307X173715
11. Kou, S. *Welding Metallurgy*, 2nd ed.; John Wiley & Sons, Inc., Hoboken, New Jersey, 2003; pp. 341-352.
12. Li, R., Wang, T., Wang, C., Yan, F., Shao, X., Hu, X., Li, J. A study of narrow gap laser welding for thick plates using the multi-layer and multi-pass method. *Opt. Laser Technol*. **2014**, 64, 172-183. https://doi.org/10.1016/j.optlastec.2014.04.015
13. Acherjee, B. Hybrid laser arc welding. *Opt. Laser. Technol*. **2018**, 99:67–71. https://doi.org/10.1016/j.optlastec.2017.09.038
14. Wei, H., Zhang, Y., Tan, L., Zhong, Z. Energy efficiency evaluation of hot-wire laser welding based on process characteristic and power consumption. *J. Clean. Prod*. **2015**, 87, 255-262. https://doi.org/10.1016/j.jclepro.2014.10.009
15. Phaoniam, R., Shinozaki, K., Yamamoto, M., Kadoi, K., Tsuchiya, S., Nishijima, A. Development of a highly efficient hot-wire laser hybrid process for narrow-gap welding-welding phenomena and their adequate conditions. *Weld World* **2013**, 57, 607–613. https://doi.org/10.1007/s40194-013-0055-1
16. Zhu, S., Nakahara, Y., Yamamoto, M., Shinozaki, K., Aono, H., & Ejima, R. Additive manufacturing phenomena of various wires using a hot-wire and diode laser. *Weld World* **2022**, 66, 1315-1327. https://doi.org/10.1007/s40194-022-01273-w
17. Shinozaki, K., Yamamoto, M., Mitsuhata, K., Nakashima, T., Kanazawa, T., Arashin, H. Bead formation and wire temperature distribution during ULTRA-HIGH-SPEED GTA WELDING using pulse-heated hot-wire. *Weld World* **2012**, 55, 12-18. https://doi.org/10.1007/BF03321281
18. Wonthaisong, S., Shinohara, S., Shinozaki, K., Phaoniam, R., Yamamoto, M. High-efficiency and low-heat-input CO2 arc welding technology for butt joint of thick steel plate using hot wire, *Q. J. Jpn. Weld. Soc*. **2020**, 38-3, 164-170. https://doi.org/10.2207/qjjws.39.96
19. Spaniol, E., Trautmann, M., Ungethüm, T., Hertel, M., Füssel, U., Henckell, P., Bergmann, J. P. Development of a highly productive GMAW hot wire process using a two-dimensional arc deflection. *Weld World* 64, **2020**, 873–883. https://doi.org/10.1007/s40194-020-00880-9
20. Suwannatee, N., Wonthaisong, S., Yamamoto, M. Shinohara, S., Phaoniam, R. Optimization of welding conditions for hot-wire GMAW with CO_2 shielding on heavy-thick butt joint. *Weld World* **2022**, 66, 833–844. https://doi.org/10.1007/s40194-021-01227-8
21. Marumoto, K., Tamata, H., Fujinaga, A., Takahashi, T., Yamamoto, H., Choi, J., Yamamoto, M. Bead shape control in high-speed fillet welding using hot-wire GMA laser hybrid welding technology, *Weld World* **2023**. https://doi.org/10.1007/s40194-023-01496-5
22. Chapter 4 - Gas Metal Arc Welding. In *Welding Handbook*, 9th ed.; O'Brien, A.; American Welding Society, 2004, Volume 2, pp. 148-197.

23. Phaoniam, R., Shinozaki, K., Yamamoto, M., Kadoi, K., Nishijima, A., Yamamoto, M. Solidification cracking susceptibility of modified 9Cr1Mo steel weld metal during hot-wire laser welding with a narrow gap groove. *Weld World* **2014**, 58, 469-476. https://doi.org/10.1007/s40194-014-0130-2